Active equalization of series/parallel Li-ion battery modules including no-load conditions.

Miguel Crespo
R&D Department
Cegasa Energía S.L.U.
Miñano, Spain
mcrespo@cegasa.com

Ramy Georgious
Electrical Engineering Dept.
University of Oviedo
Gijón, Spain
georgiousramy@uniovi.es

Pablo García
Electrical Engineering Dept.
University of Oviedo
Gijón, Spain
garciafpablo@uniovi.es

Geber Villa
Electrical Engineering Dept.
University of Oviedo
Gijón, Spain
villageber@uniovi.es

***Abstract*—In Li-ion battery systems, series and series/parallel arrangements of Li-ion modules are quite common to increase voltage levels or energy capacity. This paper proposes an equalization method for Li-ion energy systems using a voltage sharing method, under load and no-load conditions. The proposed system uses module-level DC/DC power converters both for global energy exchange and equalization. The proposed method can be easily extended to an arbitrary number of series/parallel modules and introduce a no-load equalization strategy for only series arrangements.**

I. Introduction

Li-ion batteries have become a popular solution for energy storage systems, due to their high energy density, light weight, relatively long service or high cell voltage in comparison with other electrochemical batteries alternatives as lead-acid [1]. These advantages make Li-ion battery a good choice for a variety of applications, i.e. electric cars, grid supporting devices, UPS systems or storage for DC microgrids [2]. The design of a Li-ion battery system is usually done by the assembly of Li-ion modules. Each module is built by series cells to obtain a higher level of voltage, i.e. 15 series of 3.2 V achieve a module voltage of 48 V. By the series connection of modules (string), the needed voltage is reached, while the parallel connection of strings leads to the required current capability. The most basic approach for constructing the system uses passive connection among the modules. However, due to different impedances in the connection, this can trigger unbalance problems at the modules. This problem can be worsened due to the variation of some characteristics at the cell level (State of Charge of (SoC), self-discharge rate, capacity, impedance and temperature), resulting in a cell degradation [3].

The present work has been partially supported by the European Union's H2020 Research and Innovation programme under Grant Agreement No 864459 (UE-19-TALENT-864459) and the Ministry of Science, Innovation and Universities by the Industrial Doctorates programme reference DIN2018-009853B98667264. This work also was supported by the predoctoral grants program FPU for the formation in university teaching of Spain MECD under the grant IDs FPU16/06829 and FPU16/05313.

Due to the enumerated issues, battery management systems are inevitable [4], using passive or active equalization at cell and module-level. For adjacent cell-to-cell equalization one of the most common equalizer is the Buck-Boost converter in a distributed configuration [1].

Despite cell-to-cell configurations are able to equalize the individual cells in a battery module, the series/parallel connections of modules can create unabalances among them and thefore a lost in the total energy storage capacity. This paper is focused on the balance system at module-level by modifying the control system of a high gain DC/DC converter (48/400 V) used for the transfer of the main battery power. The main characteristics for this converter are the high gain voltage, high eficiency, bidirectional capability, active/pasive equalisation and modularity. The proposed system will demonstrate its operation using two different kind of module connection: Input Series Independent Output (ISIO) [3], [5]–[7], or Input Parallel Independent Output (IPIO) [2], [4]. In the literature, the input/output ports are identified either as the battery or the dc-link. In this research, the dc-link is named as the input port. System equalization under no-load conditions is also considered as a novelty of the proposed system.

The paper is structured as follows. In Section II the ISIO configuration is shown and the different equalization methods, under load and no load, are dis- cussed. In Section III, IPIO configuration and its control is presented. Section IV presents the simulation results using PLECs. Different operating points and conditions are considered, including the equalization for both the ISIO and IPIO configurations working under load and no load consitions. Finally, in Section V, the main conclusions from the paper are listed.

II. iBatt Concept

In this document the iBatt concept is presented as a solution for the issues presented in Li-Ion batteries modules. Formed by a DC/DC Isolated High Gain converter and a Li-Ion module, Fig. 1. The DC/DC converter used for this study has been presented in [8]. For the presented simulation results, the battery model presented in [9] has been used. The dynamic equations are shown in (1)-(4) and the block diagram for the implementation can be seen in Fig. 2.

Converter topology have been analized in [8]. This converter is formed by 2 stages: interleaved synchronous rectifier and three-phase dual active bridge. For the analysis carried out here, two assumptions are considered for the DC/DC converter: 1) the dynamics of the internal current and phase control loops are assumed to be decoupled from the output voltage control being the main parameter that affect the system the current injected by the converter, Fig. 4. The converter model is controlled by a quadratic voltage control of the output capacitor (V_x) presented in Fig. 5. Since the output of the PI is directly the Power that is needed move from the capacitor to the battery, using the voltages is possible determine the current at the input and ouput of the converter.

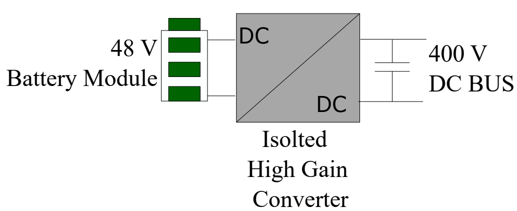

Figure 1: iBatt Concept.

$$K = \frac{(C - C_N)}{C_N}(V_{max} - V_{nom} + Ae^{-B*C_N} - 1) \quad (1)$$

$$A = V_{max} - V_{exp} \quad (2)$$

$$B = 3/C_{exp} \quad (3)$$

$$E_0 = V_{max} + K - A + R_{cell}N_{series}Id_N \quad (4)$$

Battery Module and Cell

Paramenter	Symbol	Value
Voltage Nom	V_{nom}	47.25 V
Voltage Max	V_{max}	53 V
Voltage Min	V_{min}	43 V
Capacity at nominal Voltage	C_N	162 Ah
Rated Capacity	C	180 Ah
Cell Voltage	V_{cell}	3.15 A
Cell Series	N_{series}	15
Exponetial Voltage Zone	V_{exp}	3.2 V
Capacity at Exponetial Zone	C_{exp}	5% C_R
Cell Internal Resistance	R_{cell}	0.3 mA
Nominal Discharge Current	Id_N	180 A

Table I: Battery Parameters

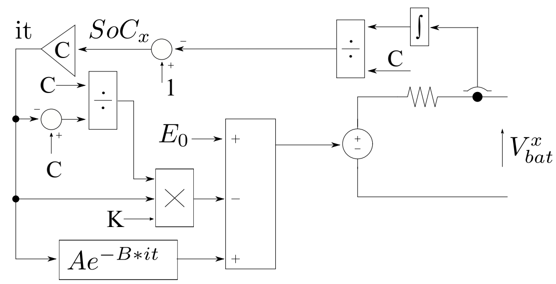

Figure 2: Battery model used for the module packs.

DC/DC ratings

Paramenter	Value
Voltage Input	400 V
Voltage Output	48 V
Max Power	18 kW

Table II: DC/DC Parameters

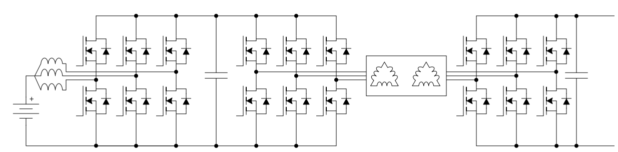

Figure 3: Proposed DC/DC converter topology according to the study developed in [8].

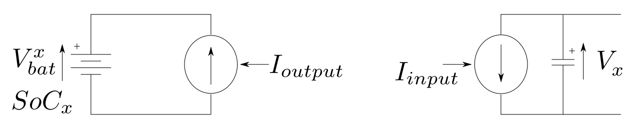

Figure 4: Lossless model.

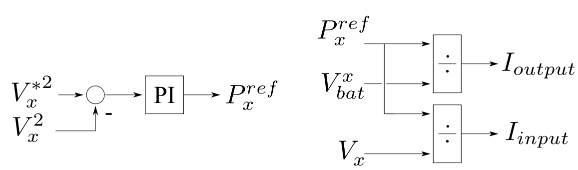

Figure 5: DC/DC voltage control.

III. ISIO CONFIGURATION CONTROL

ISIO configuration is conformed by the series connection of iBatt modules. In this paper the input of the system is the DC-link and is connected in series. And the output, Li-ion module, is isolated, forming the configuration of the ISIO, Fig. 6 a). Each iBatt module is formed by a DC/DC converter (Fig. 3)that enables the boosting of the battery voltage, 48 V, to the required level at the dc-link, 400 V.

A. Equalization under load condition

During the normal operation of the ISIO system, the input side will be connected to a load, thus demanding or delivering a current (I). The idea for the balancing system is to intentionally unbalance the voltage in the

DC link of each module by employing a droop control, [3]. The voltage unbalance induces different power exchange that, if properly controlled, will allow for the system-level equalization.

The proposed control is implemented in a central controller, which measures the SoC of each battery module. Voltage reference for the ”x” module (V_x^* where x can be every number between 1 and the number of modules, n), as is shown in Fig. 7, is obtained by adding and later filtering the equilibrium point voltage (V^{ref}), the variation of the voltage (ΔV_x) and the DC-link compensator (K^{global}/n). ΔV_x is set by a droop control for equalization purposes. With the difference between the maximum and the minimum SoCs of the ISIO (SoC_{max} and SoC_{min}), the voltage limits of the droop (ΔV^{max}) are set, Fig. 7. Then the droop is calculated as (1), where a and b parameters are calculated as (1a) (1b). Due to the bidirectional capability of the system the sign of a and b will be determined by the current, considering positive sign for the charge and negative for the discharge. However, these voltage variations affect the DC link voltage (V_{Bus}) stability. Therefore, the compensatory action is introduced. Initially, all modules operate under the same V^{ref} (2), valid at the equilibrium point where all SoCs are the same. Due to the variations introduced by the V_{Bus} droop control, positive (ΔV_{pos}) and negative

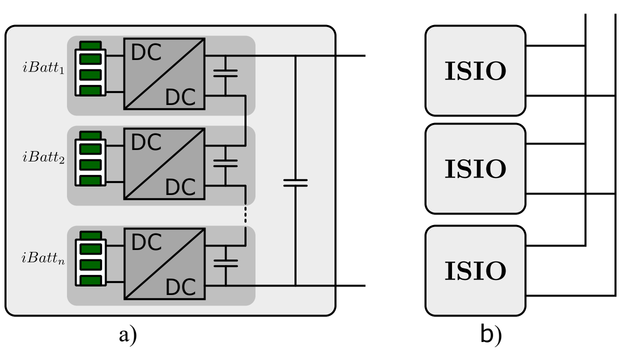

Figure 6: a)ISIO Configuration of iBatts. b) IPIO Configuration of ISIOs.

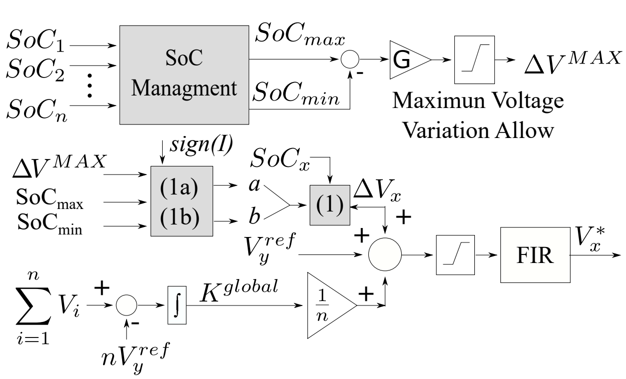

Figure 7: ISIO control scheme.

(ΔV_{neg}) terms are added to the different modules. DC link voltage is maintained when (4) is satisfied. In order to continuously meet the constraint, K^{global}, (5), is proposed. The additional voltage compensation is set by the integral controller shown in Fig. 7.

$$\Delta V_x = a \ SoC_x - b \tag{5}$$

$$a = \pm \frac{2\Delta V^{MAX}}{SoC_{max} - SoC_{min}} \tag{5a}$$

$$b = \pm \frac{SoC_{max} + SoC_{min}}{SoC_{max} - SoC_{min}} \Delta V^{MAX} \tag{5b}$$

$$V_{Bus} - nV^{ref} = 0 \tag{6}$$

$$V_{Bus} = nV^{ref} + \Delta V_{pos} + \Delta V_{neg} \tag{7}$$

$$\Delta V_{pos} = -\Delta V_{neg} \tag{8}$$

$$\Delta V_{pos} + \Delta V_{neg} + K^{global} = 0 \tag{9}$$

B. No-load equalization

During no-load operation, equalization using the proposed method is not possible due to the load current being zero. Therefore, based on the idea of active equalization presented in [10], a voltage variation is introduced by charging and discharging the DC link capacitor. During the charge state (state 1 in Fig. 8) those modules with higher capacity will impose a higher voltage than those with lower capacity. By power equivalence that will make the demanded power also smaller in the lower capacity modules. During the discharge, the opposite will occur (state 3 in Fig. 8). It is worth noting that when moving from state 1 to state 3, it is mandatory to increase the voltage of those modules with lower capacity more than those with higher capacity, so an intermediate state, state 2 in Fig. 3, is included. The same occurs when considering the 3 to 1 transition.

IV. IPIO CONFIGURATION CONTROL

In those applications requiring a higher power or energy capacity, a parallel configuration of strings will conform to an IPIO configuration. A schema for two string is shown in Fig. 6 b). Based on the proposed droop presented in [2] and [4], the control for the parallel system is implemented in an outer control loop, Fig. 9 C1. From each ISIO control loop, average SoC (SoC^{mid}) is sent to the IPIO control. Then considering the maximum and minimum SoC parameters, the droop curve is defined according to (6). In (6), I_{MAX} is given by the DC/DC nominal current. As in the previous case, a DC link compensator is added to avoid voltage variations, see (K^g) in Fig. 9.

$$\Delta V_y^{ref} = I_y + \frac{2I_{MAX}}{SoC^{MAX} - SoC^{MIN}} SoC^y_{mid} - \frac{SoC^{MAX} + SoC^{MAX}}{SoC^{MAX} - SoC^{MIN}} I_{MAX} \quad (10)$$

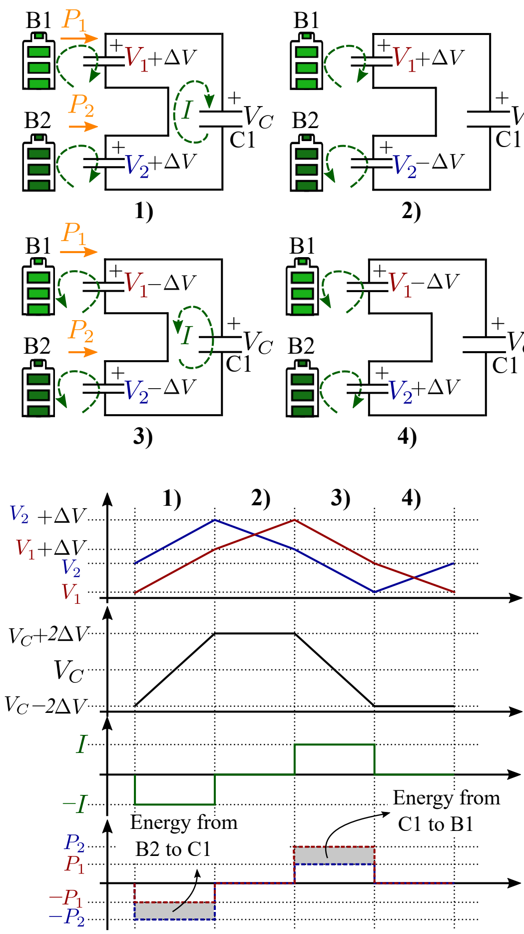

Figure 8: No load equalization.

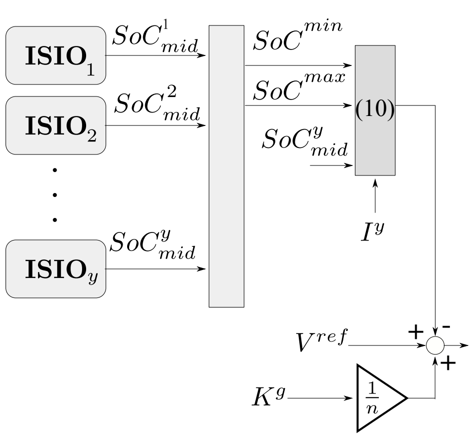

Figure 9: IPIO control scheme.

V. Simulation Results

Simulation using PLECS has been employed for validating the proposed control. For simulation tests, the battery model used is an approximation of the model presented in [8] with a lower capacity to reduce simulation times (48 V-18 Ah). In Fig. 10 The setup in which the presented simulation results are based is shown.

A. ISIO Load results

For the ISIO model, four DC/DC converters coupled to the battery model have been connected in series. Fig. 11 a) shows the SoC evolution for each module during the normal operation of the energy storage system and considering both charging and discharging conditions. Fig. 11 b) presents the variation at the DC link for each module. It can be noticed the battery voltage is limited in the band [350/450] V. These variations show the effect of the ΔV. When the system is near to the equalization, at 0.38 h, the ΔV variation becomes smaller, until it reaches the 0 value when all modules have the same SoC. Fig. 11 c) shows the demanded current. Finally, in Fig. 11 d) the effect of the proposed compensator is shown, where red and blue curves show the variation without and with the compensator respectively. As it can be seen, the system compensates for SoC unbalances of around 20 % in 20 minutes.

In Fig. 12 the control variables are shown. Fig. 12 a) shows the evolution for the maximum and minimum SoCs in the ISIO string. Fig. 12 b) shows the variation of the maximum voltage according with the SoC. Fig. 12 c) shows the compensator action K. Fig. 12 d) shows the variation calculated, previous to compensation, at each module.

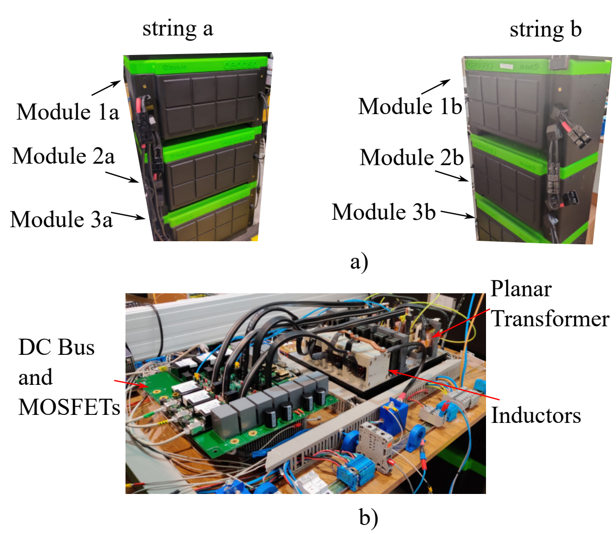

Figure 10: Experimental setup.a) The two strings of 3 baterry modules are shown for ISIO and IPIO configuration. b)DC/DC converter prototype setup.

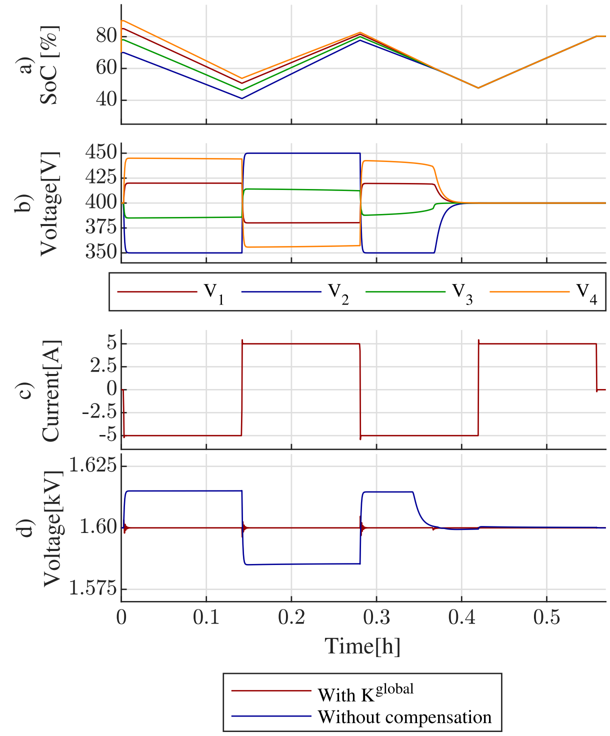

Figure 11: ISIO equalization under load conditions. a) Shows the SoC for each module. b) DC link voltage at each module. c) Load current. d) DC bus voltage.

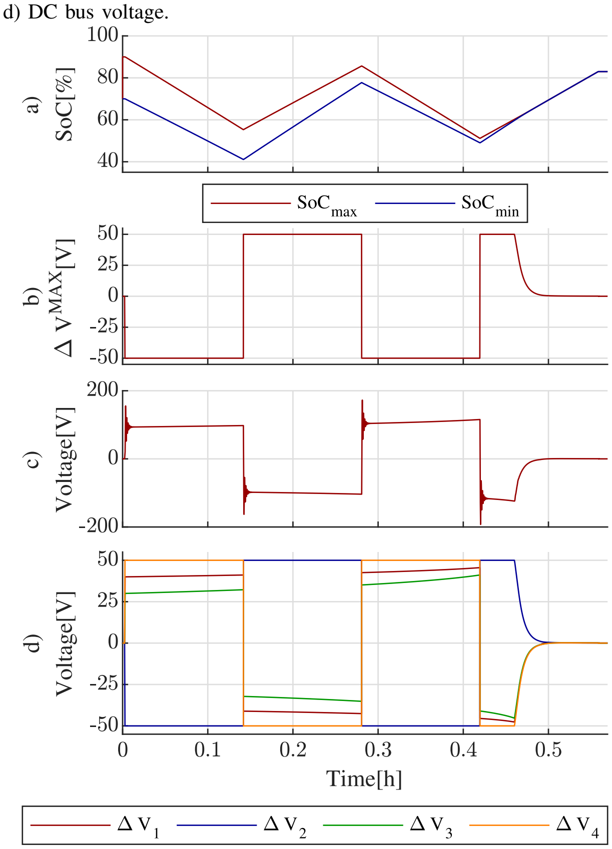

Figure 12: ISIO equalization under load conditions. a)SoC maximun and minimun. b)Maximum voltage variation, ΔV^{MAX}, c) Compensator action, K, d) Voltage variation at each module, ΔV_x.

B. ISIO No-load resuls

To evaluate the no-load case, the behaviour with two series modules has been simulated. Fig. 13 a) shows the SoC of each module and the equalization of the system. Fig. 13 b),c), d) and e) show a zoomed view for one equalization cycle. In the interval of 2.2-2.4 s the state 1 is shown, charging the output capacitor. During the next second, reference voltage of the modules is used to adjust the voltage in order to start the discharge, keeping the bus voltage stable, according with state 2. At 3.4 s the state 3 starts by discharging the capacitor and therefore charging the battery at lower capacity. Clearly, the module-level equalization is achieved, with a correction of 10

C. IPIO results

Finally, an IPIO system has been built up by two parallel strings of three series-connected modules, all of them with different SoC. Results are shown in Fig. 14, where the values of SoC, voltage and current are plotted as lines for the module a and as dashed lines for the module b. Fig. 14 a) shows SoC evolution for all modules. Fig. 14 b) shows the module-level DC link voltage. As it can be appreciated the IPIO control works in two stages. First, it imposes a sharing current until the average SoC value is achieved, (t=0.1 hours), in the different strings. Following, it forces the current to be evenly shared among the strings. Simultaneously, the ISIO control equalizes the series- modules at string levels. Fig. 14 c) shows the current at string level and the load current. Fig. 14 d) represents how the compensator action avoids voltage variation in the DC bus voltage.

In Fig. 15 the IPIO control variables for the are shown. Fig. 15 a) shows the evolution for the maximum and minimum SoC^{mid} of each string. Fig. 15 Shows the compensator action K^g. Fig. 15 c) shows the variation calculated for the current sharing, previous to compensation, at each string. At the string level, in Fig. 16 and Fig. 17 the string control variables are shown. Fig. 16 a) and Fig. 17 a) show the evolution for the maximum and minimum SoCs in each string. Fig. 16 b) and Fig. 17 b) show the variation of the maximum voltage according with the SoC. Fig. 16 c) and Fig. 17 c) show the compensator action K. Fig. 16 d) and Fig. 17 d) shows the variation calculated, previous to compensation, at each string.

From the contrast of Fig. 16 a) and Fig. 17 a) is noticed that once the string SoC equilibrium is reached, the unbalance of the parallel strings will no affect the variation of the string. Also the current sharing at Fig. 14 c), demonstrate that IPIO control is decoupled from the SoC unbalance of the strings.

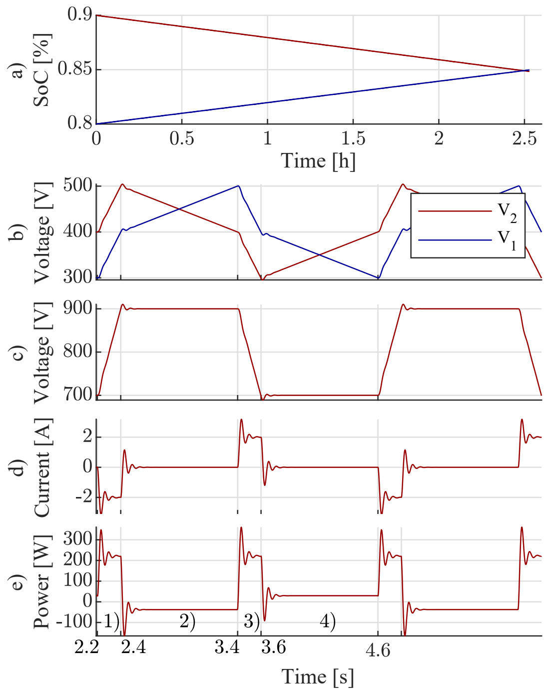

Figure 13: ISIO equalization under no-load conditions. a) SoC evolution, b) voltage of each module, c) DC bus voltage, d) current through the DC bus and d) power transmitted from the high SoC module to the low SoC module.

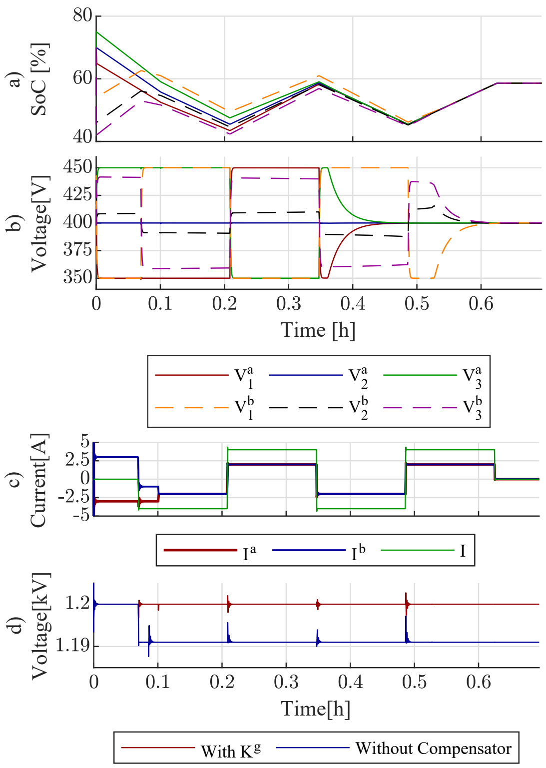

Figure 14: IPIO equalization under load and no-load conditions for 2 strings, ”a” and ”b”. a) individual module SoC, b) DC link variation, c) strings current and the load current. d) DC bus voltage with and without compensator action.

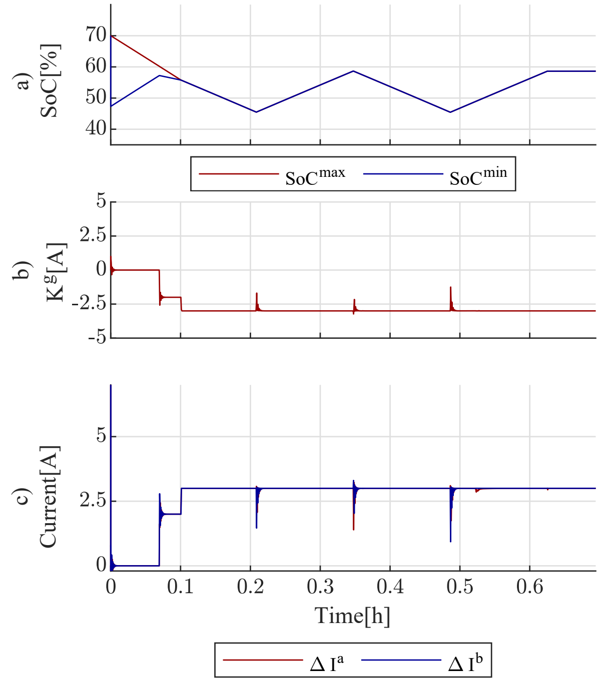

Figure 15: IPIO equalization, string a control variables. a)SoC maximun and minimun. b)Maximum voltage variation, ΔV^{MAX}, c) Compensator action, K, d) Voltage variation at each module, ΔV_x.

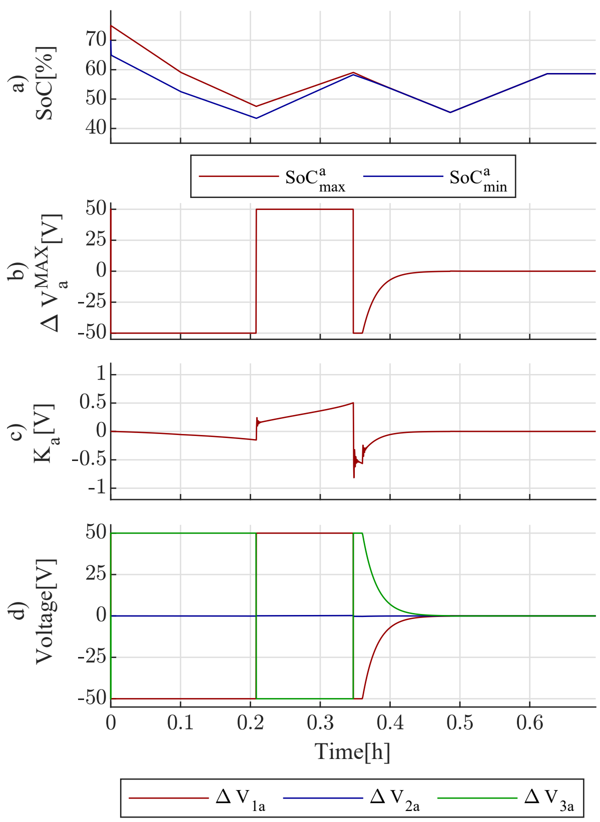

Figure 16: IPIO equalization, string a control variables. a)SoC maximun and minimun. b)Maximum voltage variation, ΔV^{MAX}, c) Compensator action, K, d) Voltage variation at each module, ΔV_x.

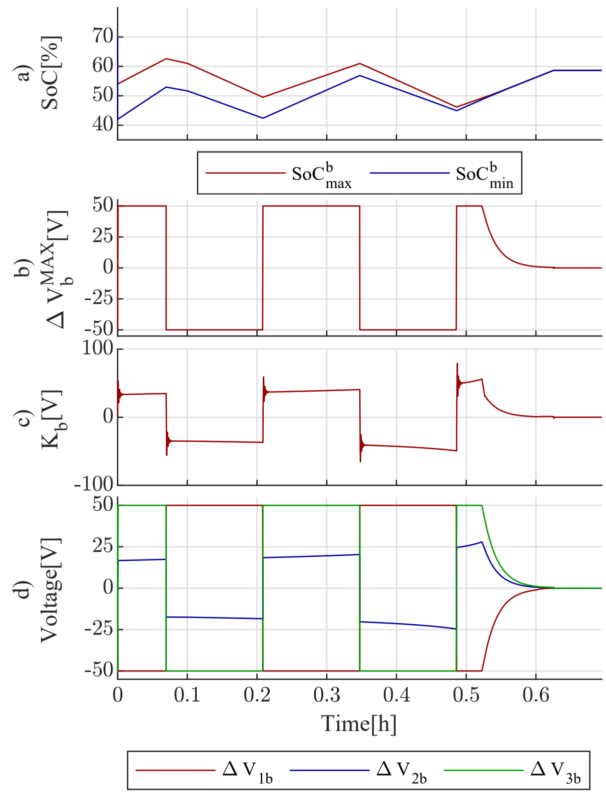

Figure 17: IPIO equalization, string b control variables. a)SoC maximun and minimun. b)Maximum voltage variation, ΔV^{MAX}, c) Compensator action, K, d) Voltage variation at each module, ΔV_x.

VI. Conclusion

In this paper, a method valid for the active equalization at module-level of Li-ion battery systems considering ISIO and IPIO configurations under load and no-load conditions has been presented. The proposed control scheme has been extensively discussed and validated by initial simulation results. The obtained results show that the control system can properly work with all the tested configurations and operating conditions.

A test bench consisting of two strings with three modules per string, as shown in Fig. 10, is currently being built for the experimental validation of the ISIO string and IPIO configuration.

References

[1] S. Hong, J. Jiang, and X. Li, "A battery management system with two-stage equalization," in *2017 29th Chinese Control And Decision Conference (CCDC)*, May 2017, pp. 4109–4113.

[2] S.-Y. Yu, H.-J. Kim, J.-H. Kim, and B. Han, "Soc-based output voltage control for bess with a lithium-ion battery in a stand-alone dc microgrid," *Energies*, vol. 9, p. 924, 11 2016.

[3] S. M. Chowdhury, M. Badawy, Y. Sozer, and J. A. De Abreu Garcia, "A novel battery management system using a duality of the adaptive droop control theory," in *2017 IEEE Energy Conversion Congress and Exposition (ECCE)*, Oct 2017, pp. 5164–5169.

[4] S. M. Chowdhury, M. E. Haque, A. Elrayyah, Y. Sozer, and J. A. De Abreu-Garcia, "An integrated control strategy for state of charge balancing with output voltage control of a series connected battery management system," in *2018 IEEE Energy Conversion Congress and Exposition (ECCE)*, Sep. 2018, pp. 6668–6673.

[5] Y. Li and Y. Han, "A module-integrated distributed battery energy storage and management system," *IEEE Transactions on Power Electronics*, vol. 31, no. 12, pp. 8260–8270, Dec 2016.

[6] W. Chen and G. Wang, "Decentralized voltage-sharing control strategy for fully modular input-series–output-series system with improved voltage regulation," *IEEE Transactions on Industrial Electronics*, vol. 62, no. 5, pp. 2777–2787, May 2015.

[7] X. Li, M. Zhu, M. Su, J. Ma, Y. Li, and X. Cai, "Input-independent and output-series connected modular dc–dc converter with intermodule power balancing units for mvdc integration of distributed pv," *IEEE Transactions on Power Electronics*, vol. 35, no. 2, pp. 1622–1636, Feb 2020.

[8] M. Crespo, P. García, R. Georgious, G. Villa, and J. García, "Design and control of a modular 48/400v power converter for the grid integration of energy storage systems," in *2019 IEEE Energy Conversion Congress and Exposition (ECCE)*, Sep. 2019, pp. 1421–1428.

[9] O. Tremblay and L. Dessaint, "Experimental validation of a battery dynamic model," *World Electr Veh J*, vol. 3, pp. 1–10, 06 2009.

[10] C. Pascual and P. T. Krein, "Switched capacitor system for automatic series battery equalization," in *Proceedings of APEC 97 - Applied Power Electronics Conference*, vol. 2, Feb 1997, pp. 848–854 vol.2.